Proceedings of CONF-MCEE 2026 Symposium: Advances in Sustainable Aviation and Aerospace Vehicle Automation
DOI: 10.54254/2755-2721/2026.KA27515

A Review of Advanced Joinery Methods for Lightweight Automotive Applications

Muyang He[1*], Xinyue Ye[2], Dihao Zhang[3], Ruizhe Cai[4], Qi Lan[5], Weihao Zhao[6]

[1]*Shenzhen College of International Education, Shenzhen, China*
[2]*School of Automotive Engineering, Shanghai University of Engineering Science, Shanghai, China*
[3]*University of California, Irvine, USA*
[4]*Nanjing Foreign Language School, Nanjing, China*
[5]*Longcheng High School, Shenzhen, China*
[6]*Changwai Bilingual School, Changzhou, China*
**Corresponding Author. Email: s23085.he@stu.scie.com.cn*

Abstract. To enhance fuel economy and minimize emissions of vehicles, a lightweight design is currently considered the most viable option by the automotive industry. This paper will investigate mechanical joints and welded joints that connect different lightweight materials for assembly. An analysis has been conducted on multiple modern joint technologies, such as bolted joints, friction stir welding, MIG welding, laser welding, ultrasonic welding, and riveting. By using a machine to test the strength in tensile and shear, it was found that MIG welding has the highest strength in the welding field, with an endurance strength of 238.3 MPa. These findings are meant to furnish engineers with ideas on how to optimize the strength-to-weight ratio of assemblies with multiple materials in vehicles, as these will promote the manufacture of lightweight, well-balanced, and energy-efficient vehicles.

Keywords: Tensile Shear Strength, Lightweight Automotive Design, Advanced Joinery Methods

1. Introduction

The automotive industry adopts a variety of technologies in response to growing pressure to make cars more fuel-efficient and reduce emissions. Lighter weight requires less energy to move. To further reduce the weight of automobiles, researchers need to study connection methods. Common connection techniques include friction welding, bolted connections, MIG welding, ultrasonic welding, laser welding, and riveting. Among them, mechanical methods such as bolts and rivets are widely used in lightweight vehicle structures. These allow disconnection, reusability, and flexible connections between different materials [1]. In contrast, welding methods—such as laser, ultrasonic, and friction welding—typically provide higher tensile strength, better sealing, and more permanent attachment [2]. Whether using mechanical fastening or welding, the joining method must match the materials' performance, thermal sensitivity, and structural reliability. Selecting the right technique is crucial to balancing strength and weight for better fuel efficiency. This study examines various

DOI: 10.54254/2755-2721/2026.KA27515

connection methods to determine how advanced joinery can enhance tensile shear strength while reducing vehicle weight, providing engineers with guidance for designing lighter, more efficient automobiles.

Friction stir welding (FSW) is widely employed in industrial production, but it still has some problems. In RS-FSW process, excessive friction produced from the rotating shoulder can reduce the best tensile strength (UTS) in the joint as a result of overheating and welding defects such as flash, ripples, and thickness variation [3,4]. Non-rotational shoulder friction stir welding (NRS-FSW) is proposed to try solving those issues. The joint is formed by using a stationary shoulder to reduce excessive heat input, surface flash, and joint inhomogeneity [3,4]. However, the NRS-FSW will limit the fractional welding speed/rate or slower welding speeds, reducing the tools' life. Thus, adoption of this approach to industry is limited [5]. Further improvement was achieved by Li et al. [6] who found that the use of threaded and grooved sleeves in refill friction stir spot welding (RFSSW) promoted downward product flow and disrupted the alclad layer, thus suppressing hook formation. Huang et al. [7] also confirmed that variations in tool geometry and some welding parameters can regulate the morphology of interfacial defects and, consequently, influence the tensile shear properties. Collectively, these findings highlight the essential significance of tool design in improving interfacial property and improving the mechanical performance of the connections.

Bolted connections are a standard mechanical joining technique in automotive engineering, as they achieve the specified performance requirements and can be applied to lightweight materials. Previous investigations have focused on the use of metal-bolt joinery in composite structures for improving mass efficiency in lightweight automotive applications. Ireman and colleagues [8] created a finite element model that replicated such mechanical properties as load distribution and abstracted failure modes in this type of composite joint. The model yielded critical pieces of information on stress magnification in bolt holes. In the study by He and Guan [9], they further showed that factors such as multi-bolt configurations and closer bolt spacing play a greater role in optimizing the load transfer efficiency of composite material assemblies. Furthermore, Herrington et al. [10] found that preload and edge stress concentration critically affect the durability of CFRP countersunk bolted joints. While bolted joints are common in composite structures, optimizing their configuration to reduce mass without sacrificing strength remains challenging. This study aims to develop a framework for reliable automotive joint design by analyzing factors such as orientation and hybrid connections.

Al/steel dissimilar joints are for lightweight structures in automotive and aerospace industries. This study investigates the impaction of strain proportion on tensile performance of laser MiG brazing aluminum/steel joints. Earlier studies have tested diverse welding techniques: Du et al. [11] examined eccentric laser welding parameters for TWIP steel/Al alloy butt joints; Chen et al. [12] used hybrid laser-CMT for steel-Al butt welding-brazing. Xie et al. [13] explored rotating laser-welded-brazed 6061 Al/304 SS joints with varying rotation speeds. Liu et al. [14] tested DP780 laser-welded joints under 1–1000 s^{-1}, finding increased tensile/yield strengths. The current study, focusing on laser-MIG welded-brazed 304 SS/6061-T6 joints with ER4043 filler (1000 W laser power, 4.5 m/min wire feed) and strain rates 1–1000 s^{-1} (reinforced) and 1–500 s^{-1} (unreinforced), builds on these by examining strain rate sensitivity specific to such joints, where key findings show reinforced joints reach 222.6 MPa at 1000 s^{-1} and unreinforced ones peak at 238.3 MPa at 500 s^{-1}.

Ultrasonic metal welding (USMW) is a connection method that uses rapid vibrations and moderate pressure to join similar or dissimilar metals without generating significant heat [15,16]. Prior studies employed ultrasonic welding to join aluminum alloy AA6111 with titanium alloy Ti-

DOI: 10.54254/2755-2721/2026.KA27515

6Al-4V, focusing on analyzing the resulting welds' microstructure and mechanical behavior [17]. Some researchers conducted ultrasonic welding on Al/Mg/Al layered clad sheets, aiming to evaluate the effectiveness of the process for joining dissimilar layered metals [18]. Other researchers found that USW offers a shorter welding cycle, typically within seconds, and requires lower clamping loads compared to FSW and F-SPR, due to acoustic softening at the interface [19]. Some scientists employed ultrasonic welding to join copper-to-copper interfaces and systematically optimized the welding parameters, aiming to enhance joint strength [20]. Besides, several investigators characterized the evolution of microstructure and evaluated the mechanical performance of extruded alloys joined by ultrasonic welding [21].

Laser welding is an important technology for lightweight design, but the high-quality connection needs to be investigated. For example, brittleness issues exist at the interface of thin plates at the joint [22]. A recent study found that introducing an alternating magnetic field during the process of welding dissimilar magnesium/steel materials can improve the weaknesses of the joint material, while nickel can generate intermetallic compositions and solid solutions with magnesium and iron, respectively [23-25]. Other researchers have found that how to improve durability of abrasion-resistant steel by controlling the mechanical properties and the phase structure [26-28]. Laser welding shows superior efficacy compared to conventional welding methods due to its narrower fusion interface region and minimized thermal degradation zone [27]. Besides, laser welding delivers minimal thermal input to the workpiece, while simultaneously achieving lower distortion, narrower weld beads, and faster welding speeds, making it a good choice for high-strength lightweight connections [28].

In terms of rivet, most of the papers have discussed the shear load or fatigue performance evaluation of the riveting lap joints [29], and there are various international standards defining the dimensions, experimental setup and the fracture mechanism of the riveting lap joints [30]. But only a few of them analyzed the changes in joint strength during one-sided tensile tests, and one of the studies showed the joint strength of SPR in the unilateral tensile tests [31]. Moreover, some of the papers talked about both tensile and shear tests together. One of the papers analyzed the tensile and shear tests for solid self-piercing riveting joints [32]. Besides that, other researchers also conducted an experiment about the joint strength of H-shaped specimens in the tensile assessments [33]. There is also one paper illustrating the strength of clinching joints strength under multi-directional loading [34].

Finally, our study reviews how advanced joinery methods—friction stir welding, bolting, MIG welding, ultrasonic welding, laser welding and riveting—influence on the tensile shear strength of automotive connections. By examining one connection type for each method across various materials, we assess structural integrity, lightweight potential, and suitability for multi-material components. Comparing performance identifies techniques that optimize the strength-to-weight ratio, reduce structural mass, and enhance vehicle fuel efficiency and overall performance.

2. Friction (stir) welding

Friction stir welding (FSW) is a solid-state joining technique for joining metals and their alloys, particularly when different materials are involved. As shown in Figure 1, the process employs a rotary tool posited on the material that generates heat through friction, in addition to the thermal energy produced by the tool’s pin through mechanical agitation. Unlike traditional fusion welding processes, FSW is performed at considerably lower temperatures, which can reduce the risk of thermal degradation and eliminate any solidification related defects [35]. Researchers are

DOI: 10.54254/2755-2721/2026.KA27515

investigating how to evaluate and improve joints' tensile strength to increase automotive fuel efficiency.

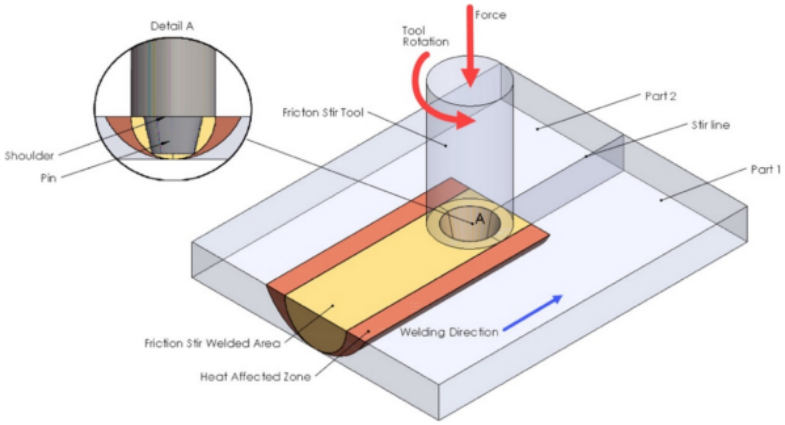

Figure 1. Graphical depiction of the friction stir welding (FSW) [36]

Recent studies on FSW focus on tooling improvements to enhance joint strength. The latest improvement, hybrid shoulder FSW (HS-FSW), shows superior tensile behavior by addressing issues of poor material flow and weak weld zones, improving aluminum alloy joints without post-weld heat treatment. To achieve this, three different tool configurations were designed and tested: RS-FSW, NRS-FSW, and HS-FSW, as shown in Figure 2. Each tool incorporated a 20 mm shoulder along with a screwed pin. Welding experiments were performed on Al-Mg-Si plates of 600 × 150 × 6 mm dimensions, using a specially built FSW machine. Welding was carried out under fixed parameters, with the tool rotating at 1800 rpm and subjected to an axial force of 8000 N. The HS-FSW configuration integrated both rotating-shoulder (RS) and stationary-shoulder (NRS) characteristics, enhancing heat generation and material flow. It is, thus, hypothesized that the HS-FSW technique will promote better grain refinement and higher tensile strength due to enhanced material stirring and optimized heat generation.

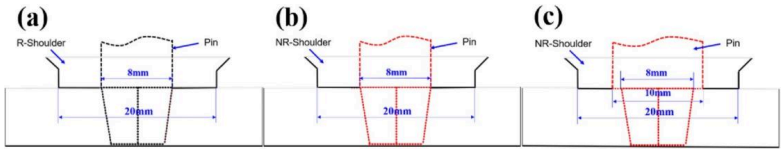

Figure 2. Demonstration of different FSW tools: (a) RS-FSW, (b) NRS-FSW, (c) HS-FSW [5]

Eventually, the study compares the strength differences between friction stir-welded Al-Mg-Si aluminum alloy joints when using three different welding tool designs in the experiment. As shown in Figure 3, we can find the peak tensile capacity of substrate metal was highest at 301 MPa. The HS-FSW joint was next in foremost tensile strength at 249 MPa, followed by NRS-FSW at 232 MPa, and RS-FSW at 197 MPa. While every joint cracked in the heat-affected zone, HS-FSW still performed best.a These findings indicate that employing a hybrid shoulder design can effectively enhance ultimate tensile capacity of welded joints [5].

DOI: 10.54254/2755-2721/2026.KA27515

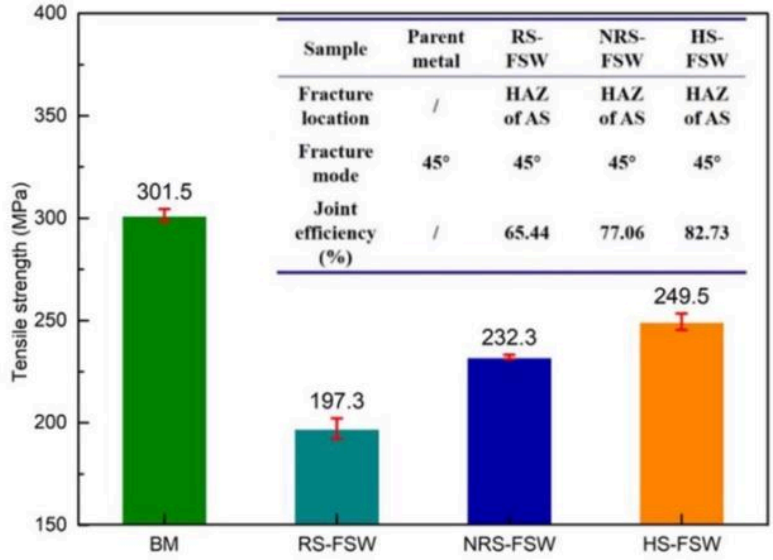

Figure 3. The comparison covered the tensile properties of four types of specimens: BM, RS-FSW joints, NRS-FSW joints, and HS-FSW joints [5]

In this work, the traditional tapered pin (T-pin) was replaced by a stepped pin (S-pin), which contributed that the tensile shear strength of FSLW joints has been significantly increased. For the best welding settings of 600 rpm rotational speed and 200 mm/min welding speed, the maximum load for tensile shear reached 7.3 kN. This improvement was largely due to the performance of the S-pin reducing hook and cold lap defects that are known to act as stress concentrators that reduce joint strength. In comparison to the T-pin welds, the S-pin produced a consequence of a more uniform weld area with less apparent defects as seen in Figure 4. Furthermore, Figure 5 presents the average tensile shear strength of FSLW joints fabricated with T-pin and S-pin tools, under welding velocities of 100–200 mm/min and rotational velocities of 300–600 rpm. It is evident that the tensile-shear load at the S-pin node is always superior to that at the T-pin node. The highest value, 7.3 kN (484 N/mm), achieved at the 600/200 condition, corresponding to a joint with a uniformly distributed hook and minimized cold lap, as depicted in Figure 5. Collectively these results indicate that the S-pin tool can be used effectively in increasing interfacial bonding and tensile shear strength in FSLW joints for nano TiB_2/2024 aluminum matrix composites [37].

DOI: 10.54254/2755-2721/2026.KA27515

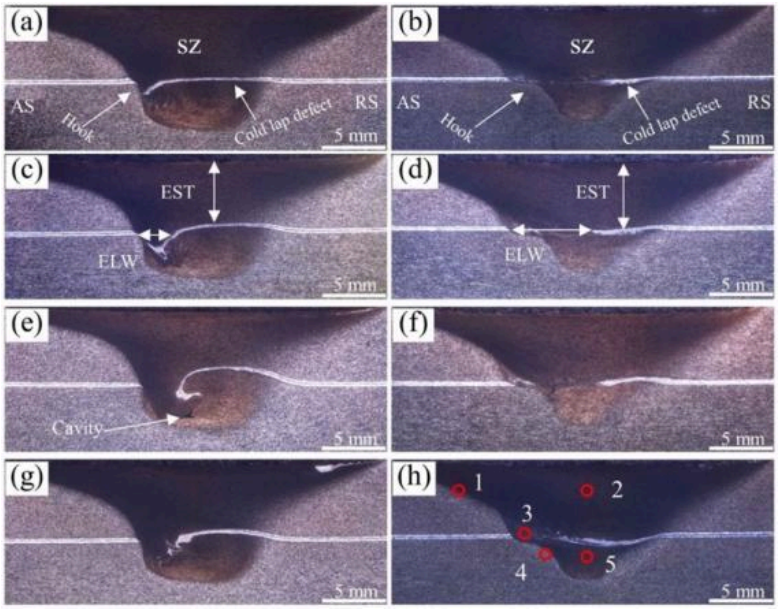

Figure 4. Macrostructural cross-section of FSLW joints made with different tool designs under various welding condition: (a, c, e, g) T-pin, (b, d, f, h) S-pin, and (a, b) 400/100, (c, d) 400/200, (e, f) 400/300, (g, h) 600/200 [37]

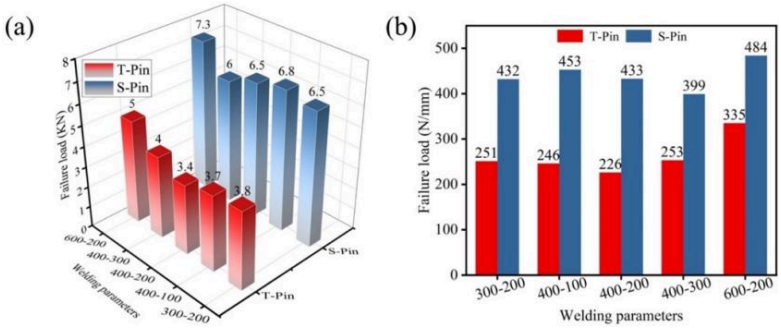

Figure 5. Tensile shear performance of FSLW joints produced using T-pin and S-pin tools under different welding conditions: (a) average tensile shear load, (b) Average force per unit width [37]

3. Bolting

Bolting is a widely used mechanical fastening method. The components being connected have holes through which the bolt is inserted, and the bolt head and nut compress the components together to form a tight joint. As shown in Figure 6 [2], typical bolted joints include bolts, nuts, washers, and clamped members such as metal plates or composite panels. The structure of the joint allows it to connect dissimilar materials in a removable and simple way. Bolted joints are valued for their reusability, ease of inspection, and compatibility with various geometries. The performance of bolted joints depends on factors such as loading conditions, joint geometry, and the potential failure modes under combined tensile and shear stresses. Researchers are currently investigating ways to enhance the strength, reliability, and material compatibility of bolted joints in lightweight automotive applications.

DOI: 10.54254/2755-2721/2026.KA27515

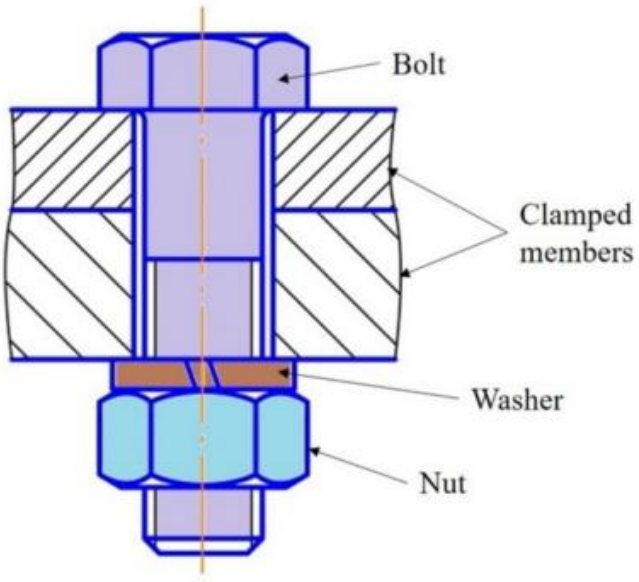

Figure 6. Main structure of bolted connections [2]

A study written by L. V. Awadhani and Anand Bewoor aims to understand the capacity of tensile shear (pulling) and compressive shear (pushing) of a composite bolted joint, and also determine its strength and stiffness. For this, they designed a set of experiments focusing on three aspects. They are the thickness of the bolts (4 mm, 5 mm, or 6 mm), the placement of the internal fibers of the carbon fiber plates (all fibers in one direction or cross-laid), and the capacity to load (0.2, 2.0, or 5.0 mm per minute). There were 18 distinct combinations of experiments, and each one was tested under both tensile and compressive conditions. As shown in Figure 7 [38], to keep the plate in place while undergoing the compression shear test and for the setup to be in the same conditions for both tests for the validity of the data, it was clamped. The trials targeted two principal variables: the maximum force a specimen can endure and stiffness. The last step was to apply the mathematical model on the results for extracting the most valuable combinations [38].

DOI: 10.54254/2755-2721/2026.KA27515

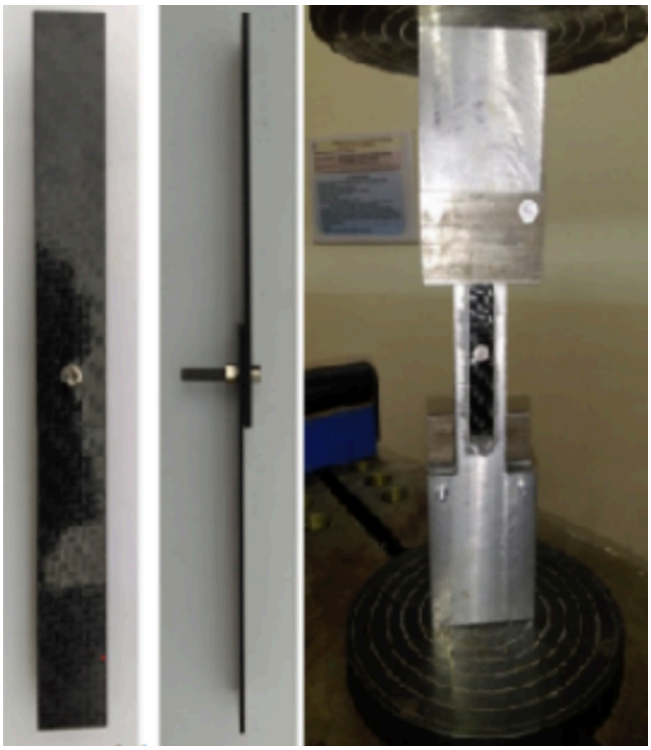

Figure 7. The experimental samples were clamped in the machine [38]

The empirical data supports the statement that the larger the bolt, the more reliable the connection. It is not only the most important but also the most influential component in our strength and rigidity. The results of the experiment are presented in Table 1. When conducting tensile tests and tensile shear tests, the level of effectiveness was highest with the use of unidirectional plates, 6 mm thick bolts, and an applied force rate of 2 mm/min. Also, a maximum tensile force of 5,374 N was recorded, which indicates a high level of stiffness. The plates with cross-laminated layers had the greatest tension force (7,852 N) and the stiffness (1,980 N/mm) in compression tests and compression shear tests. This was done through a mathematical model, and the fit reached about 94%. The researchers employed five additional experiments to confirm the model, which had a prediction error of less than 2%. Ultimately, they reached their most important goal. The core principle of bolted composite joints with high strength and stiffness is to enable their amazing reliability. That makes bolted joints an extremely powerful tool in lightweight and structural soundness design for the automotive [38].

Table 1. Data of tension-shear and compression-shear of peak load and joint stiffness [38]

Load case	Optimum parameter setting	Optimum parameter setting	Optimum parameter setting	Peak Load	Joint siffness
	L	S	d	N	N
Tension-shear	1	2	6	5374	999
Compression-shear	2	5	6	7852	1980

DOI: 10.54254/2755-2721/2026.KA27515

4. MIG welding

MIG welding functions as a semi-automatic or automatic arc welding method: it joins metals through the formation of an electric arc between a fusible wire electrode (fed continuously) and the specimen, which in turn causes local melting and resolidification of the materials. As shown in Figure 8, electrical current forms an electric arc, causing heating and melting the metal materials under the covering of inert gas, and the melted materials could form a weld pool under the high temperature [39]. Advantages of using MIG include providing high efficiency [40], good weld quality and aesthetics [41], versatility for various materials and thicknesses [42], low hydrogen content, and reduced crack susceptibility [43]. These properties make MIG welding suitable for automotive vehicle assembly, as it enables lower weight, higher performance, increased production efficiency, and greater economic value.

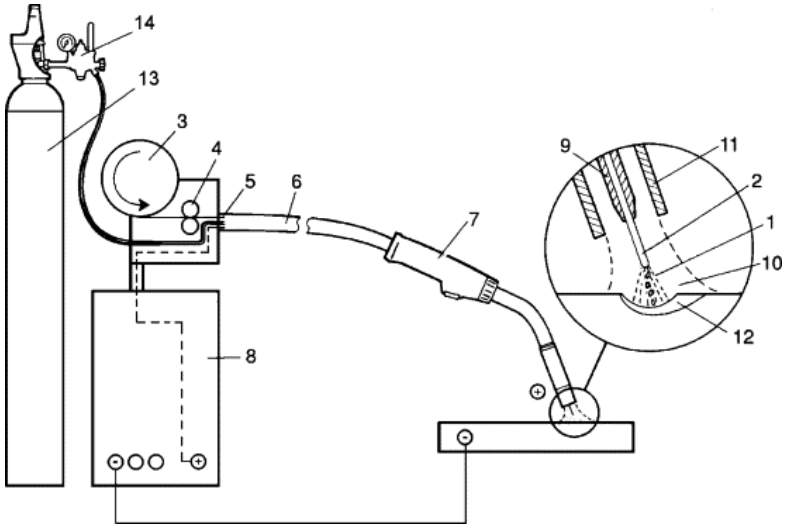

Figure 8. The working principle of MIG welding. 1. Electric Arc. 2. Electrode. 10. Shielding Gas. 11. Shielding Gas Nozzle [39]

The results, made by C. Rajendran et al in 2024, are shown in Table 2, all pulsed CMT-MIG-welded AA2014-T6 joints exhibited substandard tensile properties and hardness in comparison with the base metal, primarily due to microstructural heterogeneity and heat-affected zone (HAZ) softening; among them, STA joints achieved the highest joint efficiency (71.6%) with tensile strength of 326 MPa, yield strength of 266 MPa and elongation of 3.8% (Figure 9 shows the microhardness profiles confirming improved HAZ hardness in STA joints). Reinforced joint area is manifested in Figure 10 exhibited a notable decrease in hardness in contrast with the weld metal and base metal. Discussion revealed that STA's superior performance stemmed from finer, more uniformly distributed hardening precipitates in the weld metal, and AA and ST had minimal effects. Conclusions emphasized that STA enhanced joint strength by promoting hardening precipitates, while AW, AA and ST showed limited improvements, highlighting the critical role of post-welding thermal processing in balancing strength and ductility for AA2014-T6 welded joints [44].

DOI: 10.54254/2755-2721/2026.KA27515

Table 2. Role of PWHT in tensile behavior of AA2014-T6 alloy joints fabricated via PCMT-MIG welding [44]

Joint no.	Condition	Tensile strength (MPa)	0.2% offset yield strength (MPa)	Elongation in 50 mm gauge length (%)	Efficiency (%)
1.	AW	295	256	6.3	64.8
2.	AA	303	258	4.5	67
3.	ST	310	261	4.9	68.1
4.	STA	326	266	3.8	71.64
5.	BM	455	431	9	-

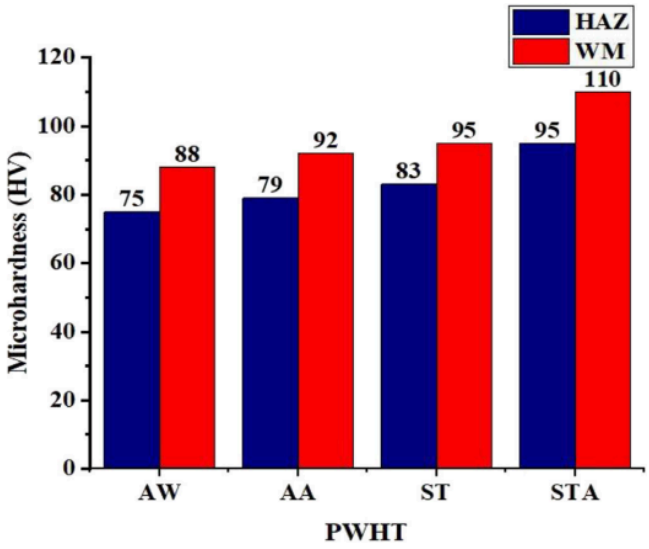

Figure 9. Microstructural hardness variations in PWHT CMT joint [44]

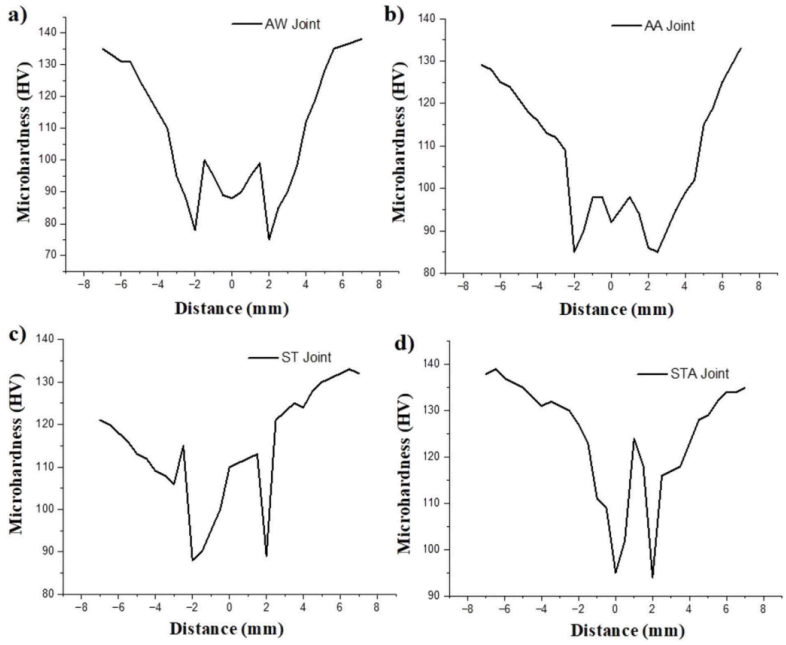

Figure 10. Variation in hardness of a) AW joint, b) AA joint, c) ST joint, and d) STA joint [44]

DOI: 10.54254/2755-2721/2026.KA27515

Y. Liu conducted relevant research in 2024, in which the laser-MIG hybrid welded-brazed method was applied to joining Al and steel. However, this research pointed out that the strain rate sensitivity of the joints obtained through this method is still limited. In contrast, this study proposes a hypothesis: joints formed by laser-MIG welded-brazing of Al and steel have high strain rate sensitivity. The principles are shown in the Figure 11 which were used to connect materials together. The materials included 2 mm thick 304 stainless steel and 6061-T6 aluminum alloy and 4043 Al-Si wire was used as the filler metal. Joints with weld reinforcement and non-reinforced weld joints were fabricated using a laser-MIG hybrid system under specific parameters (laser power 1000 W, wire feed speed 4.5 m/min, welding speed 5 mm/s, argon gas flow 25 L/min). High-speed tensile tests which are taken place in the testing machine in the Figure 12, were conducted at different strain rates. Strain distribution and fracture processes were analyzed through a strain measurement system, microstructure and fracture surfaces were examined (Figure 12) [45].

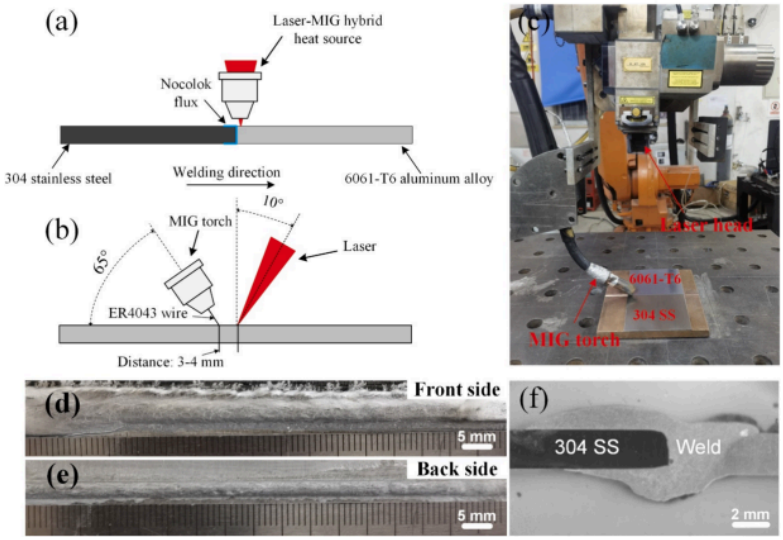

Figure 11. (a–c) Schematic diagrams of the welding operation and (d–e) visual appearances of welds in Al/steel laser-MIG welded-brazed joints [45]

DOI: 10.54254/2755-2721/2026.KA27515

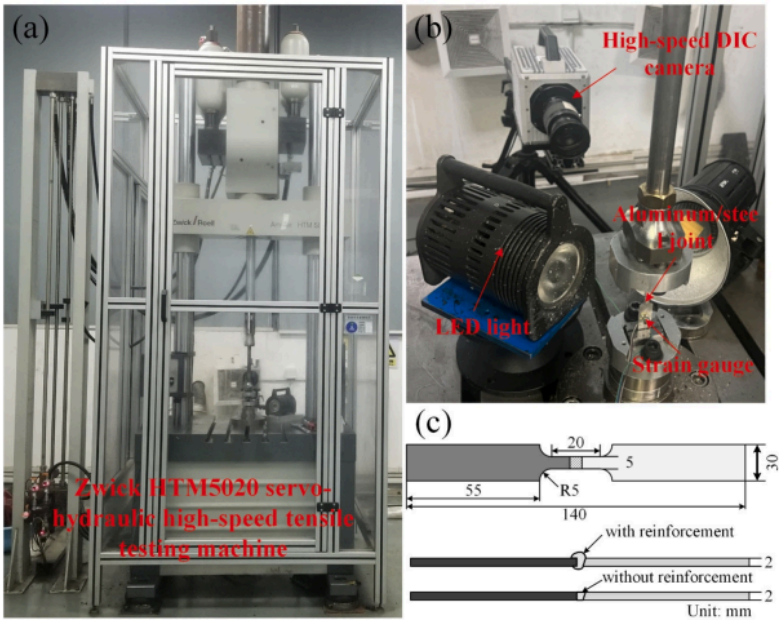

Figure 12. Illustrations of the high-speed tensile process: (a) tensile machine, (b) DIC testing setup, (c) tensile specimen dimensions and shape [45]

Figure 13 shows that for joints with weld reinforcement, fractures happened in the aluminum alloy's HAZ at lower strain proportions (1, 10 s^{-1}), showing a shear ductile fracture mode and no obvious strength change. At higher strain rates (≥100 s^{-1}), the fracture shifted to the interface: at 1000 s^{-1}, ultimate tensile strength and yield strength hit 222.6 MPa and 166.6 MPa, up by 6.5% and 17.9% from 1 s^{-1}. This strength rise came from higher defect concentration in the weld buildup and crack deflection in the IMC layer. For joints without reinforcement, all fractures were at the interface; at 500 s^{-1}, latest tensile strength arrived 238.3 MPa—58.9% higher than at 1 s^{-1}, because cracks spread slowly toward the IMC layer with Al_8Fe_2Si. Strain distribution analysis found that at higher strain rates, the strain concentration zone shifted from HAZ to interface, and fracture mode turned from ductile to mixed ductile brittle. These results clarify sensitivity to rate of deformation of laser-MIG welded-brazed Al/steel connections, offering references for safe Al/steel structure design [45].

DOI: 10.54254/2755-2721/2026.KA27515

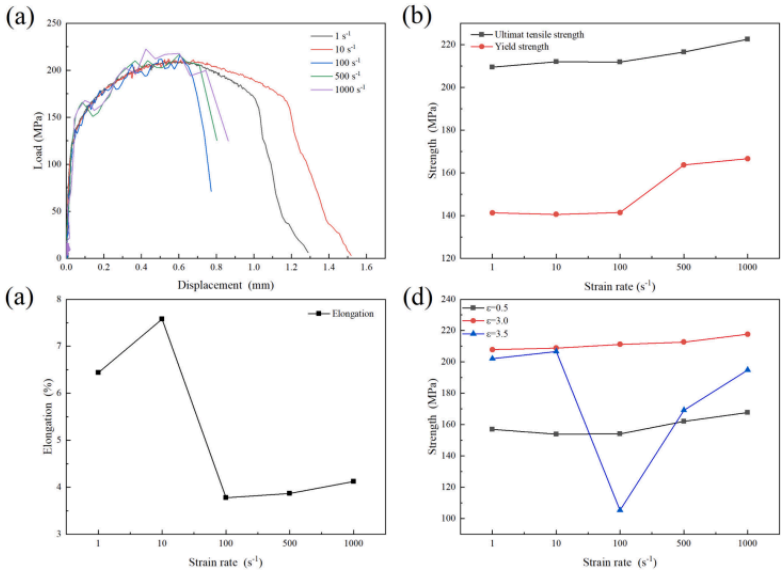

Figure 13. Properties in tension of laser-MIG welded-brazed Al/steel joints with reinforcement under different strain rates: (a) load-displacement curves, (b) strength, (c) elongation, (d) strength changes corresponding to different strain rates [45]

5. Ultrasonic welding

Ultrasonic welding is a joining tech which employs rapid vibrations to create a metallurgical bond between two workpieces held under moderate pressure. As shown in Figure 14, ultrasonic welding process relies on the conversion of vibrational energy into localized frictional heat, which softens the material surfaces and enables molecular diffusion across the joint [46]. By comparing the photos in Figure 15, it is clear that the use of ultrasonic welding leads to a refinement of the weld seam and a more uniform structure, which results in a strong and clean bond [47]. The process is especially suitable for materials with low heat conduction and is widely applied to metals and thermoplastics. Key advantages include low energy consumption, short welding cycles, minimal thermal distortion and high process repeatability. In precision manufacturing fields such as microelectronics, automotive battery assembly, aerospace and medical devices, ultrasonic welding is widely used for various connections of metal parts as shown in Figure 16 [48].

DOI: 10.54254/2755-2721/2026.KA27515

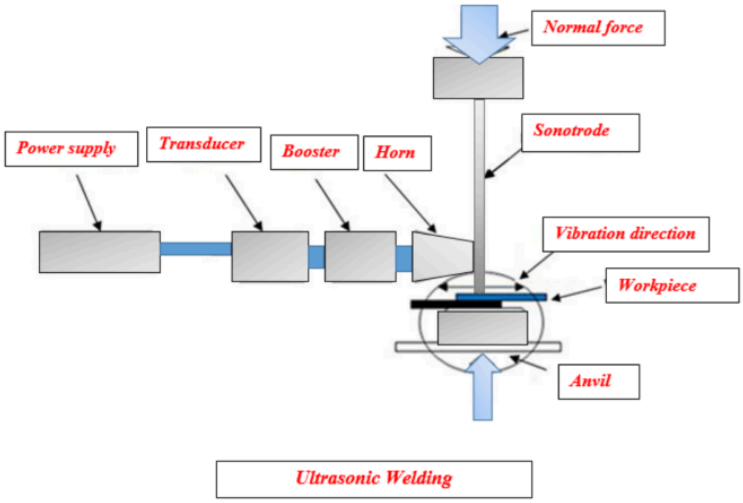

Figure 14. The working principle of ultrasonic welding [46]

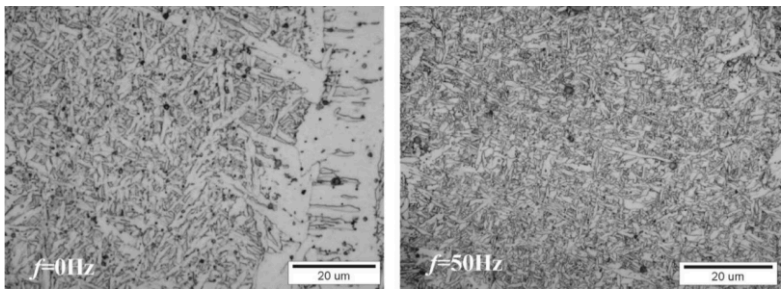

Figure 15. Microstructure of the ultrasonic welding with vibrations of 0 Hz and 50 Hz [47]

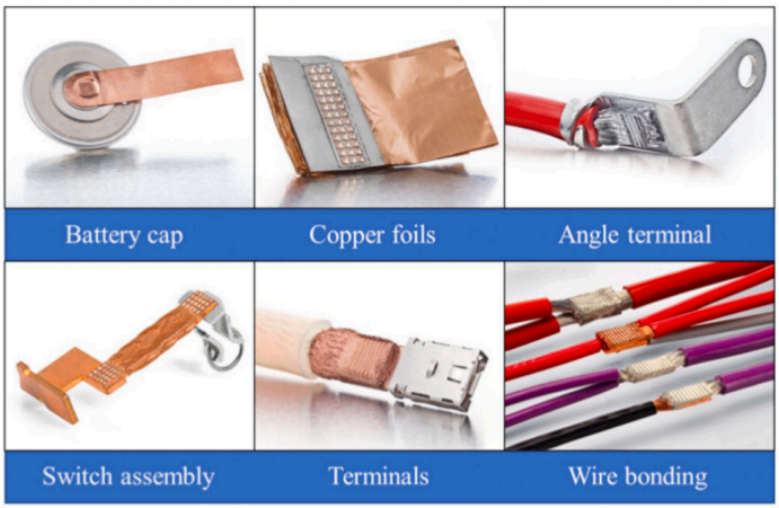

Figure 16. The applications of ultrasonic welding [48]

A study written by U. Khan, N. Z. Khan, J. Gulati investigates ultrasonic metal welding as a solid-state joining technique to bond dissimilar metals. There is the growing demand for reliable, lightweight and conductive joints in electrical applications, specifically copper and aluminum. Figure 17 illustrates the diagram of ultrasonic welding. This research is motivated by the challenge of optimizing weld strength and plasticity, particularly tensile-shear strength, which is a critical

DOI: 10.54254/2755-2721/2026.KA27515

mechanical performance metric for such joints. To achieve this, the authors systematically varied key process parameters, namely weld time, weld pressure, and amplitude, to identify optimal conditions. In the experiment, authors used 0.32mm copper and aluminum plates for ultrasonic welding with the M-4000 ultrasonic welding machine, as shown in Figure 18. Then, the shear strength of welding joints was measured at 2mm/min and the experimental parameters (welding time, pressure and amplitude) were depicted in Table 3 [15].

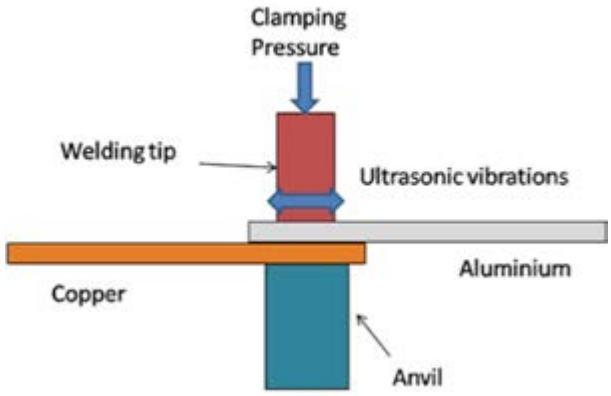

Figure 17. Schematic diagram of ultrasonic welding experiment [15]

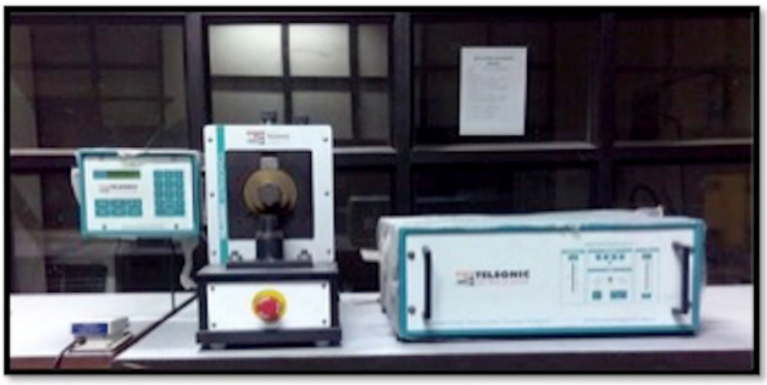

Figure 18. Ultrasonic metal welding device [15]

Table 3. Welding process parameters [15]

Factor	Symbol	Unit	Level-1	Level-2	Level-3
Welding time	A	sec	0.25	0.50	0.75
Pressure	B	bar	2	3	4
Amplitude	C	%	70	80	90

This experiment took the placement of the aluminum sheet and the copper sheet as variables and sorted the experimental data of the welded joints' surface tension shear strength into Table 4 under two variable conditions by using L9 orthogonal design. From that, it can be clearly seen that statistics of the copper plate which is placed at the top of the joint is higher than those of the aluminum one which is placed at the top. To optimize the response characteristics when copper sheet is placed at the peak, the shear strength of joint and the corresponding ratio are arranged in Table 5 in order. The results manifest that the experimental errors follow a normal distribution, as shown in

DOI: 10.54254/2755-2721/2026.KA27515

Figure 19, when the strength grows with higher welding time, pressure and amplitude. Increased pressure enhances bonding by bringing surface asperities into closer contact, enabling Van der Waals forces. Besides, longer weld time promotes molecular bonding between surfaces, while greater amplitude increases the rubbing action area, further improving bond strength. Finally, this study indicates that the best settings for the maximum tensile-shear strength (84.46 MPa) were the duration of 0.75 seconds, the pressure of 4 bar, an amplitude of 90% [15].

Table 4. L9 experimental layout assessing response variability across two treatment conditions [15]

No.	A	B	C	Tensile shear strength (Mpa)	
				Al on top	Cu on top
1	1	1	1	56.60	1.63
2	1	2	2	36.20	67.1
3	1	3	3	64.10	72.4
4	2	1	2	2.50	24.9
5	2	2	3	5.30	61.9
6	2	3	1	71.50	71.7
7	3	1	3	1.78	61.1
8	3	2	1	5.30	64.9
9	3	3	2	64.30	76.9

Table 5. L9 Taguchi orthogonal array applied to response analysis [15]

A	B	C	Tensile shear strength (Cu on top)	S/N Ratio
1	1	1	1.63	4.2438
1	2	2	67.10	36.5345
1	3	3	72.40	37.1948
2	1	2	24.90	27.9240
2	2	3	61.90	35.8338
2	3	1	71.70	37.1104
3	1	3	61.10	35.7208
3	2	1	64.90	36.2449
3	3	2	76.90	37.7185

DOI: 10.54254/2755-2721/2026.KA27515

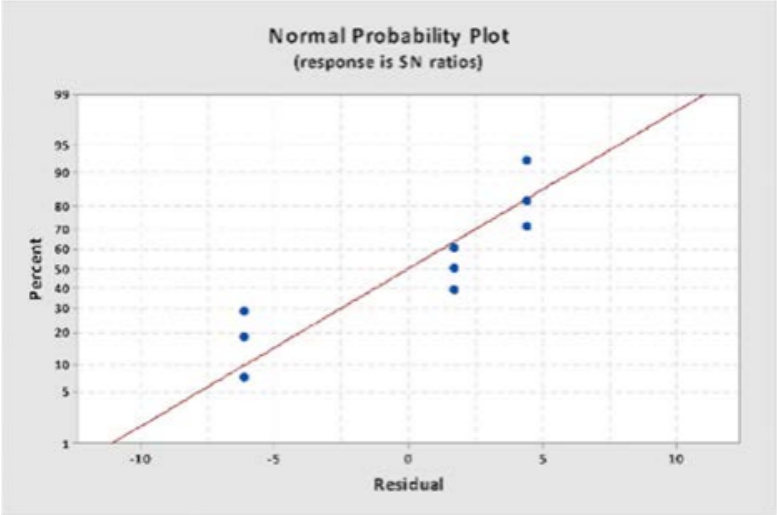

Figure 19. Plot of residuals versus theoretical normal quantiles [15]

Additional research finding written by U. Khan, N. Z. Khan, J. Gulati indicate that aluminum alloys are generally employed in high-end fields due to their numerous advantages in metal properties, such as good formability and high strength. However, this material is prone to solidification cracks and porosity during the welding process making traditional fusion welding methods unsuitable. Therefore, ultrasonic spot welding is adopted to overcome these limitations. In this paper, the authors mainly studied the tensile shear strength of ultrasonic spot-welded connections between high-strength wrought AA7075-T6 and A380 aluminum alloy with a focus on the influence of welding time (1 to 3 seconds). During the experiment, the MH-2016 ultrasonic welding machine which is shown in Figure 20 was used for welding and a 100-Hz infrared camera was employed to detect the time. Additionally, an MTS hydraulic system was utilized to do tensile shear tests at 10 mm/min. The indentation depth was evaluated using a profilometer and a microstructure, composition, and size of the post-welded material were analyzed and studied with a scanning electron microscope (SEM) at 20 kV [16].

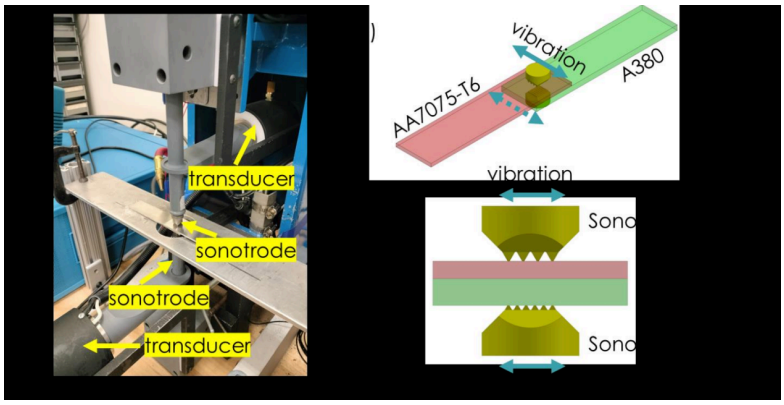

Figure 20. Experimental system for ultrasonic welding [16]

From these experiments, as illustrated in Figure 21, the peak lap shear load for welded connections with duration records of 1, 2, and 3 seconds was 5.3 kN, 6.39 kN and 6.55 kN. Besides, relative shear bonding strengths ranged from 96.29 MPa to 99.72 MPa. This improvement was attributed to an increase in the bonded area and enhanced atomic interdiffusion due to higher

DOI: 10.54254/2755-2721/2026.KA27515

temperatures and compressive stresses at the joint center. As Figure 22 demonstrated, the segments of different welded joints vary with the rise of welding time. However, further increases in welding time did not substantially improve joint strength due to potential excessive indentation and stress concentration from the sonotrode geometry. Figure 23 showed interfacial failure predominantly through the A380 side indicating stronger localized bonding on the AA7075 side despite its reduced hardness. Notably, the interfacial shear strength remained lower than the basic materials, which suggested that bonding was concentrated at the center and less uniform across the interface. Finally, it was determined that with the growth of time and temperature, the fracture behavior of all connections is interfacial fracture, which indicates that shear strength distribution along the bonding line is uneven [16].

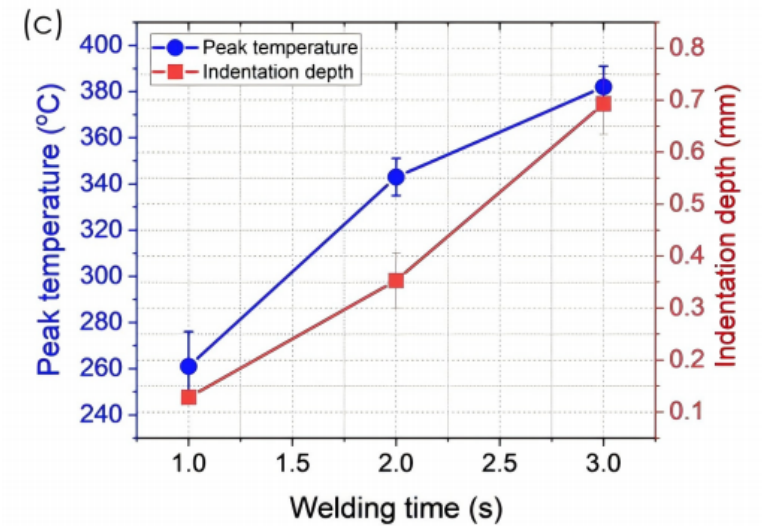

Figure 21. Maximum temperature and total mean surface indentation depth across two sheets at different welding times [16]

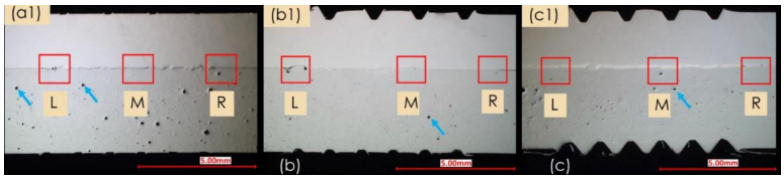

Figure 22. The cross-sectional morphologies of the joints welded at (a1) 1 s, (b1) 2 s, and (c1) 3 s [16]

DOI: 10.54254/2755-2721/2026.KA27515

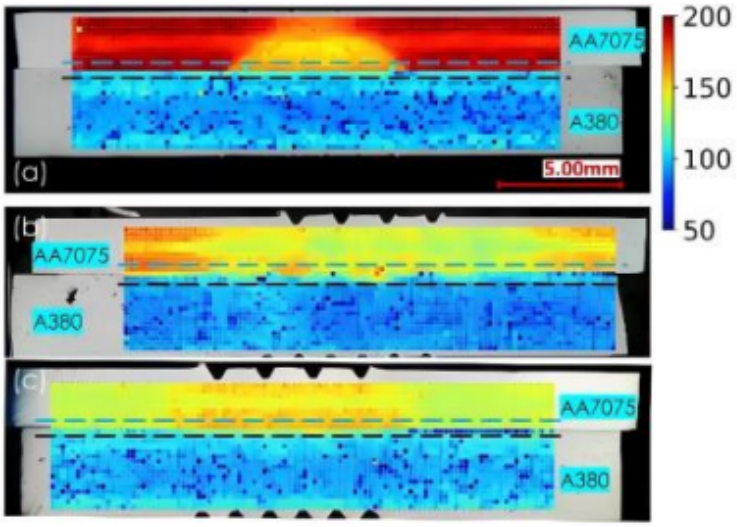

Figure 23. The hardness distribution across the joint for welding durations of (a) 1 s, (b) 2 s, and (c) 3 s [16]

6. Laser welding

In a laser welding system, a laser adds thermal energy to the substrate. The generated heat flux melts and penetrates the surface of the substrate involved in the welding process. This process results in the formation of a molten fluid pool that promotes material mixing and bonding. The laser beam welding using various material combinations is a highly effective joining technique, applicable to numerous industrial sectors, as it can achieve high-speed, flexible, and high-precision joining results [23].

To achieve energy efficiency improvements, lightweight design plays an important part in many fields. This study focuses on developing high tensile shear strength joints of Q235 low carbon steel and AZ31B Mg alloy dissimilar materials welding. In this experiment, an alternating magnetic (0.8-2.0 A every 0.2 A is an increasing unit and 15-55 Hz every 10 Hz is an increasing unit) introduced into a 6-kW fiber laser field (1250W, 20mm/s). The WDW-100 electronic universal tensile testing machine was used to conduct tensile shear tests on the joints at a tensile rate of 0.5 mm/min [24].

The result shows that at P = 1250 W, v = 20 mm s-1 the highest tensile-shear strength of steel/Mg joint without the influence of magnetic field achieved 198 MPa. In response to the excitation frequency of 35 Hz and the exciting current of 1.2 A, the joint reached a maximum σb of 228 MPa as shown in Figure 24, representing an approximate 15% enhancement compare to the field without a magnetic. As the excitation frequency and excitation current IE increased, the tensile shear strength σb first rose and then decreased. In conclusion, the application of an alternating magnetic field during laser welding increased the molten pool's motion velocity, ultimately enhancing the tensile and shear strength of joints [24].

DOI: 10.54254/2755-2721/2026.KA27515

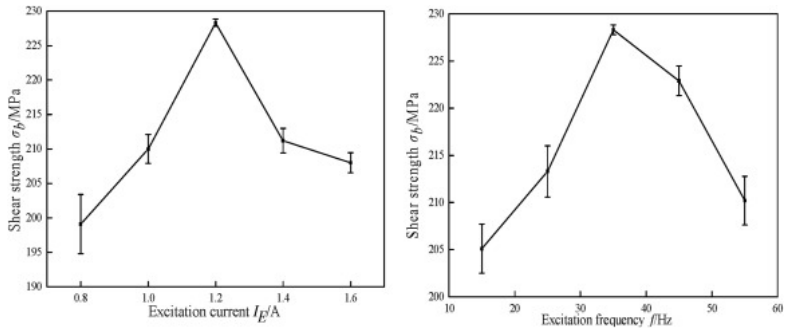

Figure 24. Variation of joint mechanical properties under alternating magnetic environment; (a) Effect of exciting current on tensile shear strength of joints; (b) Effect of excitation frequency on tensile shear strength of joints [24]

Abrasion resistant steel (ARS), a widely used extremely strong martensitic steel in extremely environments, is prone to failure under severe mechanical stresses and wear. This study enhancing the tensile shear strength of the steel lap connections to alter the weld pattern (e.g. longitudinal/transverse combined welds). The experiment used 150×50×3 mm steel plates with 50mm overlap length for the lap joints and multiple weld patterns were tested with 10 mm weld beads. Testing for tensile shear strength was performed following the standard ASTM E8/8M and using the Instron universal testing machine at 1 mm/min, with triplicate tests for each condition. A load of 0.2 kg was used for Vickers hardness measurements on weld cross-section [49,50].

As clearly presented in Figure 25, the lap joints' tensile shear strength increases significantly with weld number at constant energy input and transverse weld patterns consistently demonstrating greater shear strength compared to longitudinal weld patterns at 160 J/mm and LEIs 60. for instance, at LEI 160 J/mm, the lap joints' shear strengths of longitudinal are 275 MPa for one weld and 1110 MPa for five melds, while transverse lap joints have higher values of 370 MPa for single weld and 1170 MPa for five. This can be ascribed to the superior shear strength of the transverse weld pattern to absorb strain [50].

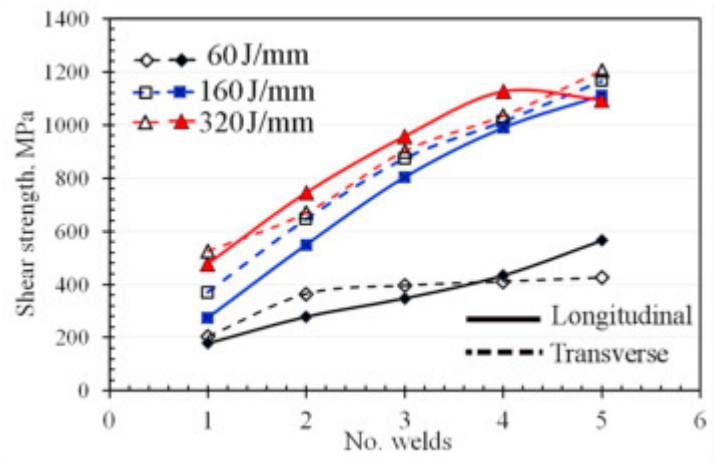

Figure 25. Dependence of the laser-welded AR600 lap joints tensile shear strength related to the laser energy inputs (60, 160, 320 J/mm), quantity of welds and positioning in the weld structures [50]

DOI: 10.54254/2755-2721/2026.KA27515

7. Rivet

A rivet is a headed pin that is used for uniting two or more components. As shown in Figure 26, after passing the shank through a hole in each piece, the other end can be pressed down to make a second head. Rivets are used widely in the vehicle industry because they are cheaply accessible, and rivets can join the components strongly. Besides that, riveting machines are able to install tons of rivets automatically [51], which helps save a lot of costs for entrepreneurs. Nowadays, with the advances of technology, many kinds of welding are combined with riveting, such as friction riveting, resistance rivet welding, and friction self-piercing riveting [52].

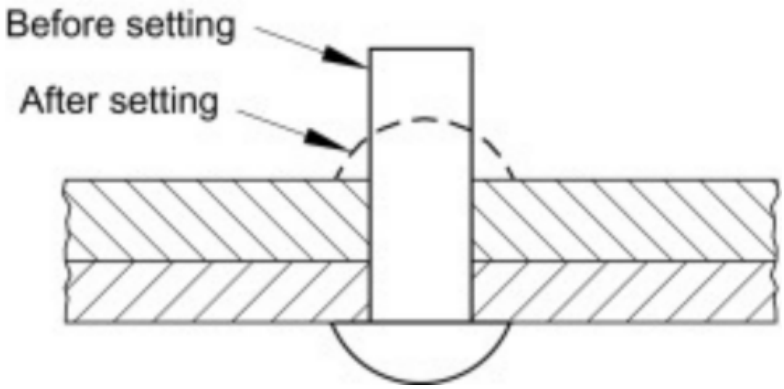

Figure 26. Rivet before and after the setting [51]

This paper talked about the relationship between the sheet material types and joint tensile capacity in tensile tests of standard joints and unique joints with solid self-piercing riveting and researchers also compared the results corresponding to the values measured in lap-joint shear tests. To do this research, four kinds of riveting joints were chosen and they are blind rivet, blind hermetic rivet, closing-up rivet and solid self-piercing riveting, as shown in Figure . The overall experiment is shown in Figure [53].

Figure 27. The four types of testing rivets: aluminum-steel BR, aluminum-steel BHR, aluminum alloy COUR, steel SSPR [53]

DOI: 10.54254/2755-2721/2026.KA27515

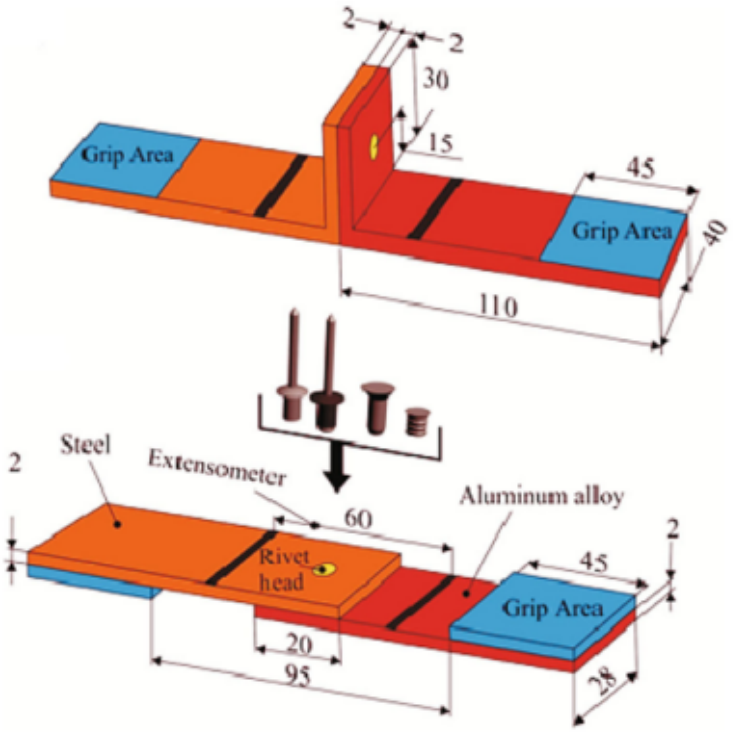

Figure 28. The specimen geometry and rivet head for two joints: T-shaped and lap [53]

The paper first discussed the failure of riveting joints in the tensile test obtained in the experiments. Although there is a specific procedure for tensile tests, they are not possible in many cases. In the one-sided tensile experimemt of T-shaped specimens, the rivet was loading at first. When it reaches a certain force, the sheets begin to bend. So, subsequent tensile loading is carried out under severe bending of the sheets.

The results that they found are:

For conventional riveting joints, in spite of the materials of joint sheet, the same status of connection strength is achieved. For the SSPR joints, the mechanical characteristics of joined sheets determine the joint strength. In tensile testing of T-shaped specimens, the rivets detach. Rivets are rotated and removed from the sheet material in shear tests [53].

8. Conclusion

This paper presents a review about the progress of advanced joinery methods, including friction stir welding, bolting, MIG welding, ultrasonic welding, laser welding, and riveting on tensile shear strength. These technological innovations offer high-quality joining solutions for lightweight automotive designs. Current research shows that each method offers distinct mechanisms for improving the tensile shear strength of joints, ranging from solid-state bonding to optimized fusion processes and mechanical interlocking. The following conclusions are about tensile shear strength improvement in advanced joinery methods.

(1) Optimization of the tool geometries, including hybrid shoulder tool design and the new stepped pin (S-pin), greatly increased the tensile shear strength in FSW processes. The hybrid shoulder FSW process produced 17% higher strength than that of rotational shoulder FSW and 6.1% higher than non-rotational shoulder FSW. Lap welding friction stir (FSLW) of nano TiB_2/2024

DOI: 10.54254/2755-2721/2026.KA27515

aluminum composites with the S-pin had a maximum fracture load of 7.3 kN based on optimal parameters.

(2) The cross connection and horizontal connections can resist a tensile force of 7852 N and 5374 N, while a compressive force of 1980 N and 999 N, respectively. These results also confirm the effectiveness of bolted connections.

(3) Al/steel laser-MIG welded-brazed joints exhibit significant strain rate sensitivity under dynamic tensile conditions, reinforced joints show strength enhancement above 100 s^{-1} due to increased dislocation density and IMC crack deflection, with tensile and yield strengths reaching 222.6 MPa and 166.6 MPa at 1000 s^{-1}, unreinforced joints achieve substantial strength improvement at 500 s^{-1} via crack propagation toward the weld-side Al_8Fe_2Si phase exhibiting a highest tensile strength of 238.3 MPa.

(4) During the process of ultrasonic spot welding, increasing welding time (1-3 s) raised the peak interface temperature (261-382 °C), which eliminated edge cracking by improving ductility and reducing defects, resulting in solid-state bonds without porosity. A layer of dynamically recrystallized (DRX) grains (up to 150 μm thick) formed in the A380 near the joint, while limited DRX occurred in AA7075 due to its large grain size and small strain. Furthermore, AA7075 remained stronger than A380 and lap shear strength increased (5.3 kN to 6.55 kN) with welding time and temperature.

(5) By incorporating an alternating magnetic field into laser welding, at first the tensile shear strength of joint rose and then declined with the increasement of excitation current and excitation frequency. The highest tensile shear strength is 228 MPa, which is about 15% greater than that without magnetic industry.

(6) The joint strength of solid self-piercing rivets (SSPR) can be optimized if high strength sheets are selected. The study showed that the representative shear force for DC01 material was found to be 5.26 kN, and that of shear force for the EN AW-5754 is 3.42 kN. Hence, the joint strength of SSPR has a deep connection with the sheet material.

This study employs tensile shear strength (TSS) in evaluating how joinery methods effectively connect lightweight parts used in car design to improve fuel economy. The data suggests that FSW, particularly the hybrid shoulder and stepped-pin designs, were the top joinery method that exhibited the best TSS performance on average (up to 7.3 kN) amongst the joinery methods. The bolted joint was the second most reliable and consistent joinery method, especially in lightweight materials, specifically AZ91 and CFRP. The riveting methods were effective as joinery methods, but performance varied considerably between methods based on the material. This study has demonstrated that TSS is an effective measure to use when evaluating and optimizing joinery methods that reduce the structural weight of vehicles for fuel economy.

References

[1] J. Feng et al., “Application of Laser Welding in Electric Vehicle Battery Manufacturing: A Review, ” Coatings, vol. 13, no. 8, Art. no. 8, Aug. 2023, doi: 10.3390/coatings13081313.

[2] D. Croccolo, M. De Agostinis, S. Fini, M. Y. Khan, M. Mele, and G. Olmi, “Optimization of Bolted Joints: A Literature Review, ” Metals, vol. 13, no. 10, 2023, doi: 10.3390/met13101708.

[3] K. N. Krishnan, “On the formation of onion rings in friction stir welds, ” Mater. Sci. Eng. A, vol. 327, no. 2, pp. 246–251, Apr. 2002, doi: 10.1016/S0921-5093(1)01474-5.

[4] D. Li, X. Yang, L. Cui, F. He, and H. Shen, “Effect of welding parameters on microstructure and mechanical properties of AA6061-T6 butt welded joints by stationary shoulder friction stir welding, ” Mater. Des., vol. 64, pp. 251–260, Dec. 2014, doi: 10.1016/j.matdes.2014.07.046.

[5] T. Zhang et al., “A hybrid shoulder to achieve a significant improvement in tensile strength and fatigue performance of friction stir welded joints for Al–Mg–Si alloy, ” J. Mater. Res. Technol., vol. 27, pp. 2280–2291, Nov. 2023, doi:

DOI: 10.54254/2755-2721/2026.KA27515

10.1016/j.jmrt.2023.10.067.
[6] Y. Li et al., “Effect of tool geometry on hook formation and mechanical properties of refill friction stir spot welding in alclad 2A12-T42 aluminium alloy, ” Sci. Technol. Weld. Join., vol. 28, no. 6, pp. 478–487, Aug. 2023, doi: 10.1080/13621718.2023.2180203.
[7] Y. Huang, L. Wan, X. Si, T. Huang, X. Meng, and Y. Xie, “Achieving High-Quality Al/Steel Joint with Ultrastrong Interface, ” Metall. Mater. Trans. A, vol. 50, no. 1, pp. 295–299, Jan. 2019, doi: 10.1007/s11661-018-5006-4.
[8] Á. Olmedo and C. Santiuste, “On the prediction of bolted single-lap composite joints, ” Compos. Struct., vol. 94, no. 6, pp. 2110–2117, May 2012, doi: 10.1016/j.compstruct.2012.01.016.
[9] M. SHAN, R. ZHANG, Y. GONG, F. LIU, L. ZHAO, and N. HU, “A characteristic curve-based numerical framework for predicting strength of multi-bolted composite joints subjected to hygrothermal condition, ” Chin. J. Aeronaut., vol. 37, no. 11, pp. 265–277, Nov. 2024, doi: 10.1016/j.cja.2024.07.029.
[10] X. Qin, X. Cao, H. Li, M. Zhou, E. Ge, and Y. Li, “Effects of countersunk hole geometry errors on the fatigue performance of CFRP bolted joints, ” Proc. Inst. Mech. Eng. Part B J. Eng. Manuf., vol. 236, no. 4, pp. 337–347, Mar. 2022, doi: 10.1177/09544054211028534.
[11] M. Du, W. Wang, X. Zhang, and J. Niu, “Effect of process parameters on performances of TWIP steel/Al alloy dissimilar metals butt joints by laser offset welding, ” Mater. Sci. Eng. A, vol. 853, p. 143746, Sept. 2022, doi: 10.1016/j.msea.2022.143746.
[12] S. Chen, S. Li, Y. Li, J. Huang, S. Chen, and J. Yang, “Butt welding-brazing of steel to aluminum by hybrid laser-CMT, ” J. Mater. Process. Technol., vol. 272, pp. 163–169, Oct. 2019, doi: 10.1016/j.jmatprotec.2019.05.018.
[13] H. Xia et al., “In situ SEM study on tensile fractured behavior of Al/steel laser welding-brazing interface, ” Mater. Des., vol. 224, p. 111320, Dec. 2022, doi: 10.1016/j.matdes.2022.111320.
[14] Y. Liu, R. Liu, Z. Zhu, Y. Li, and H. Chen, “Fracture mechanism of aluminum/steel laser-arc welded-brazed joints during quasi-static tensile and dynamic fatigue tests, ” Eng. Fail. Anal., vol. 152, p. 107461, Oct. 2023, doi: 10.1016/j.engfailanal.2023.107461.
[15] U. Khan, N. Z. Khan, and J. Gulati, “Ultrasonic Welding of Bi-Metals: Optimizing Process Parameters for Maximum Tensile-Shear Strength and Plasticity of Welds, ” Procedia Eng., vol. 173, pp. 1447–1454, 2017, doi: 10.1016/j.proeng.2016.12.210.
[16] Y. Li, J. Chen, P. Agrawal, and Z. Feng, “Microstructure and mechanical properties of ultrasonic spot welding of AA7075-T6 and A380 casting aluminum alloy, ” J. Manuf. Process., vol. 110, pp. 126–133, Jan. 2024, doi: 10.1016/j.jmapro.2023.12.061.
[17] C. Q. Zhang, J. D. Robson, O. Ciuca, and P. B. Prangnell, “Microstructural characterization and mechanical properties of high power ultrasonic spot welded aluminum alloy AA6111–TiAl6V4 dissimilar joints, ” Mater. Charact., vol. 97, pp. 83–91, Nov. 2014, doi: 10.1016/j.matchar.2014.09.001.
[18] A. Macwan, V. K. Patel, X.Q. Jiang, C. Li, S. D. Bhole, D. L. Chen, “Ultrasonic spot welding of Al/Mg/Al tri-layered clad sheets, ” Mater. Des. 1980-2015, vol. 62, pp. 344–351, Oct. 2014, doi: 10.1016/j.matdes.2014.05.035.
[19] Q. Mao, N.Coutris, H. Rack, G. Fadel, and J. J. U. Gibert, “Investigating ultrasound-induced acoustic softening in aluminum and its alloys, ” Ultrasonics, vol. 102, p. 106005, Mar. 2020, doi: 10.1016/j.ultras.2019.106005.
[20] S. Elangovan, K. Prakasan, and V. Jaiganesh, “Optimization of ultrasonic welding parameters for copper to copper joints using design of experiments, ” Int. J. Adv. Manuf. Technol., vol. 51, no. 1–4, pp. 163–171, Nov. 2010, doi: 10.1007/s00170-010-2627-1.
[21] Y. Higashi, C. Iwamoto, Y. Kawamura, “Microstructure evolution and mechanical properties of extruded Mg96Zn2Y2 alloy joints with ultrasonic spot welding, ” Mater. Sci. Eng. A, vol. 651, pp. 925–934, Jan. 2016, doi: 10.1016/j.msea.2015.11.057.
[22] “Mechanical characterization of laser-welded double-lap joints in ultra-high and low strength steels for sandwich panel applications, ” Mater. Today Proc., vol. 28, pp. 455–460, Jan. 2020, doi: 10.1016/j.matpr.2019.10.031.
[23] “Effect of tempering on the impact-abrasive and abrasive wear resistance of ultra-high strength steels, ” Wear, vol. 440–441, p. 203098, Dec. 2019, doi: 10.1016/j.wear.2019.203098.
[24] “Study on microstructure and properties of Mg/steel laser welding-brazing joint assisted by alternating magnetic field with Ni interlayer, ” Int. J. Lightweight Mater. Manuf., vol. 4, no. 4, pp. 416–422, Dec. 2021, doi: 10.1016/j.ijlmm.2021.06.002.
[25] “Two-body abrasion resistance of high carbon steel treated by quenching-partitioning-tempering process - ScienceDirect.” Accessed: July 22, 2025. [Online]. Available: https: //www.sciencedirect.com/science/article/abs/pii/S0043164819308440
[26] “Martensitic wear resistant steels alloyed with titanium - ScienceDirect.” Accessed: July 22, 2025. [Online]. Available: https: //www.sciencedirect.com/science/article/abs/pii/S0043164819312244

DOI: 10.54254/2755-2721/2026.KA27515

[27] “The effect of the initial microstructure of the X70 low-carbon microalloyed steel on the heat affected zone formation and the mechanical properties of laser welded joints - ScienceDirect.” Accessed: July 22, 2025. [Online]. Available: https: //www.sciencedirect.com/science/article/abs/pii/S0921509320311436
[28] “Laser beam welding of dual-phase DP1000 steel - ScienceDirect.” Accessed: July 22, 2025. [Online]. Available: https: //www.sciencedirect.com/science/article/abs/pii/S0924013617304557
[29] R. Matsuzaki, M. Shibata, and A. Todoroki, “Improving performance of GFRP/aluminum single lap joints using bolted/co-cured hybrid method, ” Compos. Part Appl. Sci. Manuf., vol. 39, no. 2, pp. 154–163, Feb. 2008, doi: 10.1016/j.compositesa.2007.11.009.
[30] “Standard - Eurocode 3 — Design of steel structures — Part 1-8: Joints SS-EN 1993-1-8: 2024 - Swedish Institute for Standards, SIS, ” Svenska institutet för standarder, SIS. Accessed: July 22, 2025. [Online]. Available: https: //www.sis.se/en/produkter/construction-materials-and-building/construction-industry/technical-aspects/ss-en-1993-1-82024/
[31] X. He and B. Xing, “The ultimate tensile strength of coach peel self-piercing riveting joints, ” Strength Mater., vol. 45, no. 3, pp. 386–390, May 2013, doi: 10.1007/s11223-013-9469-7.
[32] J. Mucha, “The effect of material properties and joining process parameters on behavior of self-pierce riveting joints made with the solid rivet, ” Mater. Des. 1980-2015, vol. 52, pp. 932–946, Dec. 2013, doi: 10.1016/j.matdes.2013.06.037.
[33] B. Bartczak, J. Mucha, and T. Trzepieciński, “Stress distribution in adhesively-bonded joints and the loading capacity of hybrid joints of car body steels for the automotive industry, ” Int. J. Adhes. Adhes., vol. 45, pp. 42–52, Sept. 2013, doi: 10.1016/j.ijadhadh.2013.03.012.
[34] J. Mucha and W. Witkowski, “The clinching joints strength analysis in the aspects of changes in the forming technology and load conditions, ” Thin-Walled Struct., vol. 82, pp. 55–66, Sept. 2014, doi: 10.1016/j.tws.2014.04.001.
[35] P. Kah, R. Rajan, J. Martikainen, and R. Suoranta, “Investigation of weld defects in friction-stir welding and fusion welding of aluminium alloys, ” Int. J. Mech. Mater. Eng., vol. 10, no. 1, p. 26, Dec. 2015, doi: 10.1186/s40712-015-0053-8.
[36] S. Kilic, F. Ozturk, and M. F. Demirdogen, “A comprehensive literature review on friction stir welding: Process parameters, joint integrity, and mechanical properties, ” J. Eng. Res., vol. 13, no. 1, pp. 122–130, Mar. 2025, doi: 10.1016/j.jer.2023.09.005.
[37] S. Chen, P. Niu, X. Fu, Y. Li, L. Ke, and Y. Huang, “Significant improvement in tensile shear properties of friction stir lap welded nano TiB2/2024 Al composite joints via a novel tool pin geometry design, ” Mater. Charact., vol. 214, p. 114075, Aug. 2024, doi: 10.1016/j.matchar.2024.114075.
[38] L. V. Awadhani and A. K. Bewoor, “Behavior of Composite Bolted Joint Under Tension-Shear and Compression-Shear Load Cases, ” Int. Rev. Mech. Eng. IREME, vol. 17, no. 1, p. 39, Jan. 2023, doi: 10.15866/ireme.v17i1.23002.
[39] K. Weman, “8 - MIG/MAG welding, ” in Welding Processes Handbook (Second Edition), K. Weman, Ed., Woodhead Publishing, 2012, pp. 75–97. doi: 10.1533/9780857095183.75.
[40] M. S. Kang and H. Chung, “Dynamic force balance model considering tapering effect in gas metal arc welding, ” J. Mater. Process. Technol., vol. 257, pp. 79–87, July 2018, doi: 10.1016/j.jmatprotec.2018.02.029.
[41] F. Li, W. Tao, G. Peng, J. Qu, and L. Li, “Behavior and stability of droplet transfer under laser-MIG hybrid welding with synchronized pulse modulations, ” J. Manuf. Process., vol. 54, pp. 70–79, June 2020, doi: 10.1016/j.jmapro.2020.02.017.
[42] J. Wang et al., “Hybrid transfer learning and GAN-driven approach for online detection of welding defects, ” J. Manuf. Process., vol. 135, pp. 82–99, Feb. 2025, doi: 10.1016/j.jmapro.2024.12.039.
[43] B. Gülenç, K. Develi, N. Kahraman, and A. Durgutlu, “Experimental study of the effect of hydrogen in argon as a shielding gas in MIG welding of austenitic stainless steel, ” Int. J. Hydrog. Energy, vol. 30, no. 13, pp. 1475–1481, Oct. 2005, doi: 10.1016/j.ijhydene.2004.12.012.
[44] C. Rajendran et al., “Enhancing tensile properties of pulsed CMT–MIG welded high strength AA2014-T6 alloy joints: Effect of post weld heat treatment, ” Int. J. Lightweight Mater. Manuf., vol. 7, no. 2, pp. 344–352, Mar. 2024, doi: 10.1016/j.ijlmm.2023.10.004.
[45] Y. Liu, Y. Li, Z. Zhu, and H. Chen, “Effect of strain rate on tensile characteristics and failure behavior of Al/steel welded joint producing by a laser-MIG composite heating source, ” Eng. Fail. Anal., vol. 164, p. 108689, Oct. 2024, doi: 10.1016/j.engfailanal.2024.108689.
[46] S. Tilahun, M. D. Vijayakumar, C. Ramesh Kannan, S. Manivannan, J. Vairamuthu, and K. P. Manoj Kumar, “A Review On Ultrasonic Welding of Various Materials and Their Mechanical Properties, ” IOP Conf. Ser. Mater. Sci. Eng., vol. 988, no. 1, p. 012113, Dec. 2020, doi: 10.1088/1757-899x/988/1/012113.

DOI: 10.54254/2755-2721/2026.KA27515

[47] A. Krajewski, P. Kołodziejczak, P. Cegielski, and J. Grześ, “Support with mechanical vibrations of welding processes review of own research, ” Weld. Technol. Rev., vol. 93, no. 3, pp. 57–73, Aug. 2021, doi: 10.26628/wtr.v93i3.1143.

[48] X. M. Cheng, K. Yang, J. Wang, W. T. Xiao, and S. S. Huang, “Ultrasonic system and ultrasonic metal welding performance: A status review, ” J. Manuf. Process., vol. 84, pp. 1196–1216, Dec. 2022, doi: 10.1016/j.jmapro.2022.10.067.

[49] W. Guo, Z. Wan, P. Peng, Q. Jia, G. Zou, and Y. Peng, “Microstructure and mechanical properties of fiber laser welded QP980 steel, ” J. Mater. Process. Technol., vol. 256, pp. 229–238, June 2018, doi: 10.1016/j.jmatprotec.2018.02.015.

[50] “Optimization of the tensile-shear strength of laser-welded lap joints of ultra-high strength abrasion resistance steel, ” J. Mater. Res. Technol., vol. 11, pp. 1434–1442, Mar. 2021, doi: 10.1016/j.jmrt.2021.01.121.

[51] P. R. N. Childs, “16 - Fastening and power screws, ” in Mechanical Design Engineering Handbook (Second Edition), P. R. N. Childs, Ed., Butterworth-Heinemann, 2019, pp. 773–832. doi: 10.1016/B978-0-08-102367-9.00016-0.

[52] J. Wu, C. Chen, Y. Ouyang, D. Qin, and H. Li, “Recent development of the novel riveting processes, ” Int. J. Adv. Manuf. Technol., vol. 117, no. 1, pp. 19–47, Nov. 2021, doi: 10.1007/s00170-021-07689-w.

[53] J. Mucha and W. Witkowski, “Mechanical Behavior and Failure of Riveting Joints in Tensile and Shear Tests, ” Strength Mater., vol. 47, no. 5, pp. 755–769, Sept. 2015, doi: 10.1007/s11223-015-9712-5.